1 Radial Dirac equation (spherical potentials)

Using atomic units[1], the Dirac equation is (e.g., [1])

$$(H_D - \varepsilon)\,\phi(\boldsymbol{r}) = 0, \tag{1}$$

where H_D is the Dirac Hamiltonian:

$$H_D = c\boldsymbol{\alpha}\cdot\boldsymbol{p} + c^2(\beta - 1) + \hat{V}, \tag{2}$$

and $\boldsymbol{\alpha} = \gamma^0\boldsymbol{\gamma}$ and $\beta = \gamma^0$ are Dirac matrices. Note that we have subtracted the electron rest energy, so the total relativistic energy is $E = \varepsilon + c^2$ (for positive total energy/electron states). For bound states, $\phi \to 0$ as $r \to \infty$ and ϕ is regular everywhere and thus normalisable. The set of solutions $\{\phi_i\}$ (including the negative energy/positron states) to (1) form a complete orthogonal set/basis. We use the standard normalisation choice, so that $\langle\phi_i|\phi_j\rangle = \delta_{ij}$.

Wavefunctions for many-electron atoms are formed from single-particle orbitals, see, e.g., Ref. [2]. For spherically symmetric potentials $\hat{V}$, we can express the four-component single-particle orbitals in the form[2,3]:

$$\phi_{n\kappa m}(\boldsymbol{r}) = \frac{1}{r}\begin{pmatrix} f_{n\kappa}(r)\,\Omega_{\kappa m}(\boldsymbol{n}) \\ ig_{n\kappa}(r)\,\Omega_{-\kappa,m}(\boldsymbol{n}) \end{pmatrix}, \tag{3}$$

where $\kappa = (l-j)(2j+1)$ is the Dirac quantum number, and Ω is a (two-component) spherical spinor,

$$\Omega_{\kappa m} \equiv \sum_{s_z=\pm1/2} \langle l, m-s_z,\, 1/2, s_z | j, m\rangle\, Y_{l,m-s_z}(\boldsymbol{n})\,\chi_{s_z}, \tag{4}$$

with $\langle j_1 m_1 j_2 m_2|JM\rangle$ a Clebsch-Gordon coefficient, Y_{lm} a spherical harmonic, $\boldsymbol{n} = \boldsymbol{r}/r$, and χ_{s_z} is a spin eigenstate [$\chi_{1/2} = (1,0)^T$, $\chi_{-1/2} = (0,1)^T$]. The components of ϕ are orthonormal according to the rules:

$$(n\kappa|n'\kappa) \equiv \int (f_{n\kappa}f_{n'\kappa} + g_{n\kappa}g_{n'\kappa})\,\mathrm{d}r = \delta_{n'n} \tag{5}$$

$$\langle\kappa m|\kappa' m'\rangle \equiv \int \left(\Omega^\dagger_{\kappa m}\Omega_{\kappa' m'}\right)\mathrm{d}\Omega = \delta_{\kappa'\kappa}\delta_{m'm}. \tag{6}$$

In this case, we can define the radial Dirac equation (a pair of coupled first-order ODEs):

$$(H_r - \varepsilon)\,F_{n\kappa} = 0, \tag{7}$$

where we defined the "radial spinor"

$$F_{n\kappa} = \begin{pmatrix} f_{n\kappa}(r) \\ g_{n\kappa}(r) \end{pmatrix}, \tag{8}$$

and "radial Hamiltonian"

$$H_r = \begin{pmatrix} \hat{V} & c(\frac{\kappa}{r} - \partial_r) \\ c(\frac{\kappa}{r} + \partial_r) & \hat{V} - 2c^2 \end{pmatrix}. \tag{9}$$

Note that the 3D Hamiltonian can also be expressed in this form simply by replacing κ in (9) with $-\hat{k}$ (top right) and $\hat{k}$ (bottom left), where $\hat{k} \equiv -1 - \boldsymbol{\sigma}\cdot\boldsymbol{l}$, and $\hat{k}\Omega_{\kappa m} = \kappa\Omega_{\kappa m}$. I will suppress the r subscript and use $(H-\varepsilon)\,F = 0$ and $(H-\varepsilon)\,\phi = 0$ interchangeably, since there is no risk of confusion. Equation (7) is often written in the equivalent form:

$$\begin{aligned} \left(\hat{V} - \varepsilon\right) f - c\left(g' - \frac{\kappa}{r}g\right) &= 0, \\ \left(\hat{V} - 2c^2 - \varepsilon\right) g + c\left(f' + \frac{\kappa}{r}f\right) &= 0. \end{aligned} \tag{10}$$

[1] $\hbar = m_e = e = |e| = 1$, $c = 1/\alpha \approx 137$

[2] We use the Dirac basis; see Appendix C.

[3] Our notation differs from some other places: compared to Ref. [1] we have $f \leftrightarrow g$; compared to [3] we have $f_{\text{here}} = P_{\text{Johnson}}$, $g_{\text{here}} = -Q_{\text{Johnson}}$; compared to Ref. [4] we have $g_{\text{here}} = \alpha g_{\text{Dzuba}}$.

1.1 Nuclear and electron potentials

For a many-electron atom, the potential term consists of the sum of the nuclear and inter-electron potentials:

$$\hat{V} = V_{\text{nuc}} + V_{\text{el}}. \tag{11}$$

The electron potential,

$$V_{\text{el}} = \sum_{i<j} \frac{1}{|\boldsymbol{r}_i - \boldsymbol{r}_j|}, \tag{12}$$

involves a huge number of terms and must be taken into account approximately. The methods used to approximate this term will be described in the following sections. For a point-like nucleus, $V_{\text{nuc}} = -Z/r$; in reality, the nuclear charge is distributed across the finite-size nucleus, and this must be taken into account.

To form V_{nuc}, we assume the nuclear charge is distributed according to a Fermi distribution,

$$\rho(r) = \rho_0\,(1 + \exp[(r-c)/a])^{-1}, \tag{13}$$

where ρ_0 is the normalisation factor, ($\int \rho\,\mathrm{d}V = Z$), c is the half-density radius, and a is defined via the 90–10% density fall-off $t \equiv 4a\ln 3$ (known as the "skin thickness"), which we take to be $t = 2.3\,\text{fm}$ for all heavy isotopes. The half-density radius is related to a and r_{rms}, the root-mean-square charge radius, as $c = \sqrt{(5r^2_{\text{rms}} - 7\pi^2a^2)/3}$. Then, V_{nuc} is obtained numerically from (13) using Gauss' law.

The code also allows you to assume a spherical nucleus:

$$V^{\text{sphere}}_{\text{nuc}}(r) = \begin{cases} -Z\dfrac{3r^2_{\text{nuc}} - r^2}{2r^3_{\text{nuc}}} & r < r_{\text{nuc}} \\ -Z\dfrac{1}{r} & r \geq r_{\text{nuc}} \end{cases} \tag{14}$$

(with $r_{\text{nuc}} = \sqrt{5/3}r_{\text{rms}}$), which is mainly used for testing.

2 Numerical solutions to the Dirac equation

2.1 Bound-state solution to local Dirac equation

Rearranging Eq. (7), we can express the single-particle radial derivative as:

$$\partial_r F = \frac{1}{c}\begin{pmatrix} -c\dfrac{\kappa}{r} & (\varepsilon - \hat{V} + 2c^2) \\ -(\varepsilon - \hat{V}) & c\dfrac{\kappa}{r} \end{pmatrix} F, \tag{15}$$

which has the familiar form of an ODE. We solve this equation using a multi-step method. The specific method used (Adams-Moulton method[4]) is described in detail in the textbook Ref. [3].

In general, Eq. (15) will have solutions for any given ε. However, we are interested in the specific bound state solutions, in which $F \to 0$ as $r \to \infty$, and $F(0) = 0$. To solve the bound-state problem, an initial ε is guessed, and the DE is solved using the multi-step method. Then, small adjustments are made to ε until (a) we have the correct boundary conditions, and (b) we have the correct state $(n\kappa)$ determined by the number of nodes of the orbital $(n - l - 1)$.

In order to use the multi-step method, a few initial points of the radial F function are required. These are determined

[4] In the code, we can use the method of order 5 to 8 (default is 5; changing makes essentially no difference) – must be set at compile time.

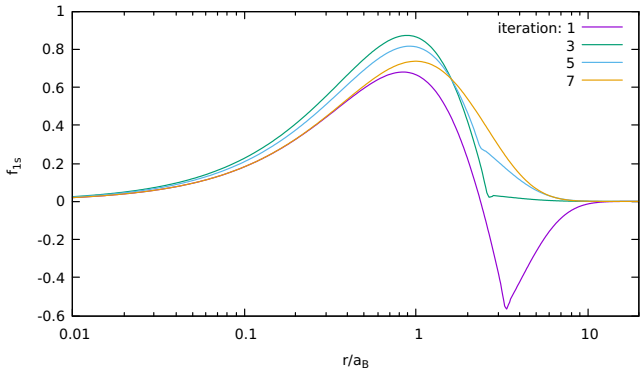

Figure 1: Hydrogen 1s orbital, as calculated at the first though 7th iteration. For this example, the initial energy guess was -0.3au, and converged to $-0.500006566..$ to parts in 10^{-16} in 12 iterations.

by solving the asymptotic form of the Dirac equation analytically accounting for the boundary conditions. It is common to expand the orbital around $r = 0$ to start the procedure, and then adjust the energy until $F \to 0$ at infinity.

A more numerically stable approach, however, is to solve the DE twice, once starting from $r = 0$, and once from $r = \infty$ [3]. These two solutions are stepped inwards toward some central point, where the two solutions are joined – one of the two solutions is re-scaled so that $f_0 = f_\infty$ at the defined point. Small energy adjustments are made until the lower g components also match at this point (this ensures the derivatives match, and the join is smooth). In our case, the two solutions are not joined at a single point, but are instead "meshed" across a few ($\simeq 5$) points around the classical turning point, defined via $V(r_{\rm ctp}) = \varepsilon$ (this is slightly different from Ref. [3]). The meshing procedure acts to smooth out numerical noise, and makes the method more numerically stable. This procedure typically allows convergence of the energies to parts in 10^{16}; see Fig. 1 for an example.

Note that Eq. (15) does not determine the normalisation for F, so the solutions must be normalised explicitly [Eq. (5)]. Further, the sign of F is also arbitray from Eq. (15); we choose $f(r)$ to be positive as $r \to 0$, as is standard.

Everywhere in the code, the fine structure constant is replaced with: $\alpha \to \lambda\alpha_0$ (in atomic units, $\alpha = 1/c$), where $\alpha_0 \approx 1/137$. The factor λ is a run-time input option, that is 1 by default. For example, letting $\lambda \to 0$ (i.e., $c \to \infty$) allows us to perform calculations in the non-relativistic limit. This is a particularly useful option for checking the calculations, and for determining the sensitivity of particular observables to variations in the fine structure constant. Modifications can also be made to the above equations to account for the finite electron/nucleus mass (reduced mass) – but this is not implemented in the code.

2.2 Radial grid

The equations must be solved numerically on a finite radial grid (the orbitals are stored in arrays on this grid). We define a grid on the region from r_0 to $r_{\rm max}$, that has N points.

Typically, we do not want to use a uniformly spaced grid, since the wavefunctions vary very rapidly at small distances, but rather slowly at large distances. We define a non-uniformly-spaced radial grid (r_i) in terms of a uniformly spaced u grid $(u_{i+1} = u_i + \delta u)$. In this case, integrals become:

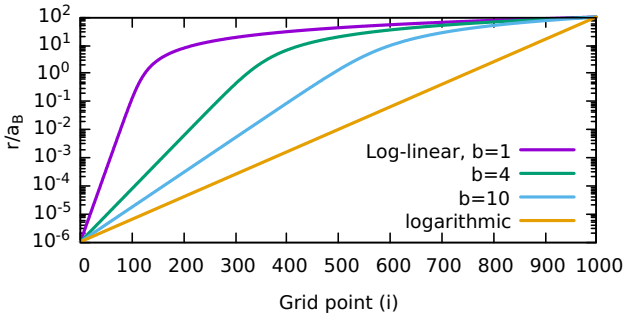

Figure 2: Radial distance r_i as function of grid-point, i.

$$\int_0^\infty f(r)\,\mathrm{d}r \to \int_{r_0}^{\mathrm{r_{max}}} f(r)\,\mathrm{d}r \to \int_{u_0}^{u_{\rm max}} f(r(u))\frac{\mathrm{d}r}{\mathrm{d}u}\,\mathrm{d}u, \quad (16)$$

which numerically becomes:

$$\int_{u_0}^{u_{\rm max}} f(r(u))\frac{\mathrm{d}r}{\mathrm{d}u}\,\mathrm{d}u \to \sum_{i=0}^{N-1} f(r_i)\frac{\mathrm{d}r}{\mathrm{d}u}\Big|_i \delta u \quad (17)$$

(in the code we actually use an n-point quadrature integration formula for the integrals). The initial/final grid points, and the grid spacings, must be chosen such that the above numerical approximations are sufficiently accurate.

In the code, we can set either a logarithmic grid, defined:

$$u = \ln(r), \qquad \frac{\mathrm{d}r}{\mathrm{d}u} = r, \quad (18)$$

or a mixed log-linear grid, defined:

$$u = r + b\ln(r), \qquad \frac{\mathrm{d}r}{\mathrm{d}u} = \frac{r}{r+b}, \quad (19)$$

which is approximately logarithmic at small distances ($r < b$), and approximately linear at large distances (typically $b \simeq 4$ au); see Fig. 2. The logarithmic grid works very well, and allows good convergence without requiring a large number of points, but works less well for highly excited states, and works quite poorly for continuum states with high energy. The log-linear grid works well in a wide range of cases, but often needs more grid points to achieve the same numerically accuracy[5].

2.3 Dirac equation involving inhomogeneous or non-local terms (Green's Method)

This is a brief overview only; for explanations/proofs see, e.g., Ref. [5]. Consider the inhomogeneous Dirac equation, with extra 'source' term S:

$$(H_1 - \varepsilon)\,F = S, \quad (20)$$

where H_l is a Dirac Hamiltonian involving only local potential terms. We solve this for a normalisable F using the Green's method for ODEs. First, take the homogeneous equation:

$$(H_1 - \varepsilon)\,G = 0, \quad (21)$$

which we solve (for a given energy ε) using the regular linear ODE multi-step methods from Sec. 2.1. Note that since F is

[5] The code also allows the use of linear grid – but this requires a very large number of points to work, so should only be used for testing.

a normalisable solution to (20) G will *not* (in general) be a normalisable solution to (21). Instead, we seek two solutions, which are each bound by one of the boundary conditions; i.e., one solution that satisfies the boundary condition at the origin, G_0, and a second that satisfies that at infinity, G_∞. Then, from the Green's method, a solution to (20) can be expressed:

$$F(r) = G_\infty(r) \int_0^r \frac{G_0(r')^T\, S(r')}{c\, w(r')}\, \mathrm{d}r' r' + G_0(r) \int_r^\infty \frac{G_\infty(r')^T\, S(r')}{c\, w(r')}\, \mathrm{d}r' \quad (22)$$

($A^T B \equiv f_A f_B + g_A g_B$) where the Wronskian,

$$w(r) = f_\infty(r) g_0(r) - f_0(r) g_\infty(r), \quad (23)$$

should be independent of r [the extra c factor in the denominator is pulled from the definition of the derivative (15) and can be included in w].

Note that this method clearly doesn't work if $w = 0$; worse, the method can be numerically unstable if S and w are both small (if S is too small, it implies the $G_{0,\infty}$ solutions will be similar, and thus w will be small).

2.4 Continuum orbitals

We are sometimes interested in continuum orbitals that are regular at the origin (see, e.g., Ref. [1]). For continuum orbitals of the desired energy $\varepsilon > 0$, we solve using the multi-step method described above, starting from the origin and integrating outwards. Note that we do not have $\phi_c \to 0$ at large r, and continuum orbitals cannot be normalised as above. For most problems, however, we do require normalised orbitals.

We choose energy normalisation [1]:

$$\int_{\varepsilon-\delta\varepsilon}^{\varepsilon+\delta\varepsilon} \langle \varepsilon' \kappa m | \varepsilon \kappa m \rangle \, \mathrm{d}\varepsilon' = 1. \quad (24)$$

This equation cannot be used directly. Instead, the orbitals are normalised in analogy with analytic Coulomb (H-like) continuum states. For Coulomb potentials, at large r we have:

$$f(r) \approx \sqrt{\frac{\alpha}{\pi\beta}}\, \sin(kr + \ldots), \quad (25)$$

with

$$\beta = \sqrt{\frac{\varepsilon}{\varepsilon + 2/\alpha^2}}$$

(other terms in sine function are either constant, or logarithmic in r). At large r, the atomic potential is also Coulomb-like, so we can use (25) to normalise the orbitals by enforcing the amplitude of the sine-like orbitals at large r to be the same as the H-like case.

To do this, we have to extend the radial grid out to very large distances, often much larger than the normal grid used to solve the bound-state orbitals. The orbital is solved out to large r until the amplitude/frequency of the oscillations becomes close enough to constant, and then the amplitude is re-scaled to match (25). After solving, the orbital is only kept up until $r_{\max}$, since larger distances typically do not contribute to any required radial integrals.

3 Hartree-Fock (self-consistent field method)

For any general "self-consistent field method", we start with an initial approximation for the electronic potential (e.g., Thomas-Fermi potential, or a simple parametric potential), and use this to generate a set of orbitals for the desired subset of atomic electrons (e.g., the core). The total electron density formed from these orbital tells us the electronic charge distribution across the atom, which we use to generate a new electronic potential (Gauss' law). In general, this new potential will be a better approximation for the true electronic potential than the initial guess. Form a new set of orbitals in this better potential, which will therefore be a better set of orbitals, which we use to generate a better-yet guess for the potential and so on, until convergence is reached. At the end, the potential used to form the electron orbitals should be the same as the potential that is formed from the electron orbitals, and is thus self-consistent.

3.1 Relativistic Hartree-Fock method

The specific method we use for this is the relativistic Hartree-Fock method, which includes the electron exchange interaction. This section largely follows the detailed explanation from Ref. [3], with a few extensions.

By minimising the many-body energy for the single Slater-determinant electronic wavefunction (see textbook [3] for details), the Hartree-Fock potential can be derived as

$$\hat{V}_{\rm HF}\phi_a(\boldsymbol{r}_1) = \sum_{i\neq a}^{N_c} \left(\int \frac{\phi_i^\dagger(\boldsymbol{r}_2)\phi_i(\boldsymbol{r}_2)}{|\boldsymbol{r}_{12}|} \mathrm{d}^3\boldsymbol{r}_2\, \phi_a(\boldsymbol{r}_1) - \int \frac{\phi_i^\dagger(\boldsymbol{r}_2)\phi_a(\boldsymbol{r}_2)}{|\boldsymbol{r}_{12}|} \mathrm{d}^3\boldsymbol{r}_2\, \phi_i(\boldsymbol{r}_1) \right), \quad (26)$$

where the sum over i extends over all occupied electrons $i = \{n_i, \kappa_i, m_i\}$. The Coulomb integrals are computed by expanding r_{12}^{-1} in terms of spherical harmonics (Laplace expansion) – see Appendix A. Integrating over angles, and summing over m quantum numbers we have:

$$\hat{V}_{\rm HF}F_a(r) = \left(\sum_b [j_b] x_b\, y^0_{bb}(r) \right) F_a(r) - \frac{1}{[j_a]} \sum_b \tilde{x}^a_b \sum_k (C^k_{ab})^2\, y^k_{ab}(r) F_b(r) \quad (27)$$

$$\equiv V_{\rm dir}(r)\, F_a(r) + [\hat{V}_{\rm ex}F_a](r), \quad (28)$$

where now the b sum extends over all occupied *orbitals* (i.e., $b = \{n_b, \kappa_b\}$), y^k_{ab} is a symmetric Coulomb integral,

$$y^k_{ab}(r) = \int_0^\infty \frac{r^k_<}{r^{k+1}_>} \left[f_a f_b + g_a g_b \right](r')\, \mathrm{d}r', \quad (29)$$

with $r_< = \min(r, r')$, and C^k_{ab} is the angular factor,

$$C^k_{ab} \equiv \langle \kappa_a || C^k || \kappa_b \rangle = (-1)^{j_a+1/2} \sqrt{[j_a][j_b]} \times \begin{pmatrix} j_a & j_b & k \\ -1/2 & 1/2 & 0 \end{pmatrix} \pi(l_a + l_b + k). \quad (30)$$

Here, $\pi(x) = 1$ if x is even, but $= 0$ if x is odd, and $[x] = 2x+1$. The x_b term is the occupation fraction for shell b, and $\tilde{x}^a_b = x_b$ when $b \neq a$, but $\tilde{x}^a_a = 1$ ($x_b = 1$ for closed shell; this is

an approximate way for treating HF equations for open-shell systems[6]).

The Hartree-Fock method is the ideal starting point for many-body calculations, since all first-order corrections to the HF potential (i.e., corrections involving single core excitations) cancel exactly [2]. The lowest-order corrections to energies and wavefunctions therefore only arise at the second-order of perturbation theory.

Hartree-Fock algorithm:

- Use a local approximation (guess) for $V_{\rm el}(r)$[7] to form an initial set of core orbitals
- Begin HF routine:
  - Form new $V_{\rm dir}$, Eq. (27)
  - For each orbital
    - Form new $V_{\rm exch}\phi$, Eq. (27)
    - Guess new energy based on change in V
    - Solve inhomogeneous Dirac Equation (Sec. 3.2)
    - Adjust energy until ϕ is eigenstate (Sec. 3.3)
    - Damp orbitals (and/or potentials)
  - Define $\epsilon_{\rm HF} = |(\varepsilon_{new} - \varepsilon_{\rm old})/\varepsilon_{\rm new}|$
  - Continue HF routine until $\epsilon < \epsilon_{\rm cut}$ for all states
- HF (core) has converged. "Freeze" $V_{\rm dir}$ and orbitals $\{\phi_c\}$
- Do HF for each valence state (from "For each orbital")

In the actual code, we perform the HF procedure for the core twice, first using an approximate localised form of the exchange potential $V_{\rm exch}$ (this first run is iterated until $\epsilon \lesssim 10^{-5}$, but doesn't need to be continued until complete convergence). This extra step is not necessary, and is only done to speed up the convergence (it provides more realistic orbitals as a starting point for the non-local HF equations). The approximate potential will be shown in Sec. 3.4. Plots of the electron density ($\rho = \sum_n |\psi_n|^2$) for Cs are shown in Fig. 3, as calculated in the Hartree-Fock and Hartree (no exchange) approximations, and using the local Green's parametric potential [6], which is used as the HF starting potential.

The HF procedure converges to the level of $\epsilon \simeq 10^{-13}$. The resulting core orbitals are correct eigenstates (that is, the energy calculated in the HF routine is the same as $\langle\phi|H|\phi\rangle$) to the level of $\sim 10^{-11}$; see Table 1. The HF orbitals are also correctly orthogonal to better than $\sim 10^{-6}$; e.g., for Cs, the orthogonality for the worst core-core and valence-valence states are calculated: $\langle 5s_{1/2}|2s_{1/2}\rangle \simeq 2\times10^{-6}$ and $\langle 7s_{1/2}|6s_{1/2}\rangle \simeq 1\times10^{-7}$.

3.2 Solving the HF equation for given orbital

To solve the HF equation for a given orbital, we use the Green's method as outlined above. The HF Hamiltonian is split in to local and non-local parts as $H_{\rm HF} = H_{\rm l} + V_{\rm nl}$, with

$$H_{\rm l} = H_0 + V_{\rm nuc} + fV_{\rm dir}, \tag{31}$$
$$V_{\rm nl} = (1-f)V_{\rm dir} + V_{\rm exch}. \tag{32}$$

Here,

$$f = \begin{cases} (N_c-1)/N_c & \text{core} \\ 1 & \text{valence} \end{cases} \tag{33}$$

is chosen so that $V_l = V_{\rm nuc} + fV_{\rm dir} \to -Z_{\rm ion}/r$ as $r\to\infty$ (otherwise, we would have $V_l \to 0$). This is done to ensure the existence of the homogenous solution that is regular at infinity (G_∞), and so that the asymptotic behaviour of the "G" (homogenous) solutions (21) more closely match that of the final solution.

Then, the inhomogeneous equation has the form of Eq. (20):

$$(H_{\rm l} - \varepsilon)\,F = -V_{\rm nl}F. \tag{34}$$

Note that the "source" term in this case contains the solution F. So the equations must be solved iteratively, with some starting approximation for the source term, so that the solution at the nth step depends on the approximate solution from the previous step. Further, $V_{\rm nl}$ and H_l also depend on the solution F via (28), and these are also formed at the nth step using $F^{(n-1)}$. That is, the equation we solve at each step of the iterative procedure is

$$\left(H_0 + V_{\rm nuc} + fV_{\rm dir}^{(n-1)} - \varepsilon\right)F^{(n)} = -\left((1-f)V_{\rm dir}^{(n-1)} + V_{\rm exch}^{(n-1)}\right)F^{(n-1)}. \tag{35}$$

The energy guess used for the $(n+1)$th step can be approximated as $\varepsilon^{(n)} + \delta\varepsilon$, with

$$\delta\varepsilon \approx \frac{\langle F^{(n-1)}|\Delta V|F^{(n)}\rangle}{\langle F^{(n-1)}|F^{(n)}\rangle} \tag{36}$$

where $\Delta V = V_{\rm HF}^{(n)} - V_{\rm HF}^{(n-1)}$. Instead of storing $F^{(n-1)}$ and $V_{\rm HF}^{(n-1)}$ for each iteration, we use $F^{(0)}$ and calculate the energy guess with respect to $\varepsilon^{(0)}$.

In general, these solutions will not be correct eigenstates of the HF Hamiltonian and therefore won't be correctly normalised. We therefore must make small adjustments to the

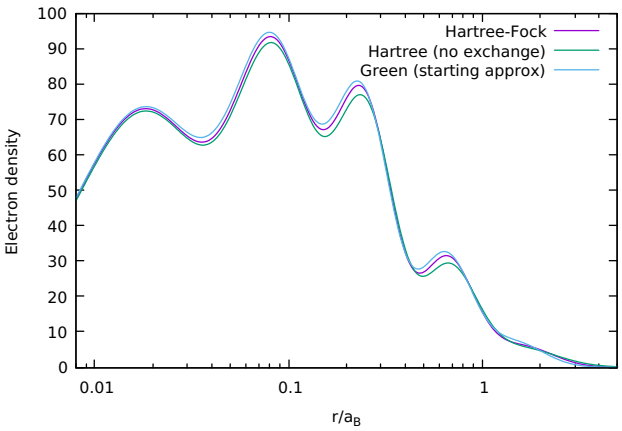

Figure 3: Electron density $\rho = \sum_n |\psi_n|^2$ for Cs in the Hartree-Fock, Hartree, and local Green potential approximations.

[6] The i sum in (26) includes a sum over all occupied m states; for partially filled shells, this doesn't include all m values. So, to do the sum, we assume each m is filled with equal probability – i.e., that each m is partially filled. We assume non-relativistic filling (e.g., $p_{1/2}$ and $p_{3/2}$ on equal footing).

[7] Essentially any approximation will do, so long as the combined nuclear and electronic potentials have $V(r\to0) \approx -Z/r$, and $V(r\to0) \approx -\xi/r$, where $\xi = 1$ for a neutral atom. I use a simple two-parameter Green's Potential [6].

Table 1: Comparison of Hartree-Fock energies with expectation value of Hamiltonian for Cs (test of numerical accuracy).

ψ	$\langle\psi\|H\|\psi\rangle$	$\varepsilon_{\rm HF}$	ϵ^*	ψ	$\langle\psi\|H\|\psi\rangle$	$\varepsilon_{\rm HF}$	ϵ
$1s$	−1330.11874784318	−1330.11874784821	-4E-12	$4d_{3/2}$	−3.48561893015	−3.48561893030	-4E-11
$2s$	−212.56445398158	−212.56445398576	-2E-11	$4d_{5/2}$	−3.39690162346	−3.39690162364	-5E-11
$2p_{1/2}$	−199.42945475153	−199.42945475392	-1E-11	$5s$	−1.48980540326	−1.48980540357	-2E-10
$2p_{3/2}$	−186.43656610582	−186.43656610730	-8E-12	$5p_{1/2}$	−0.90789795941	−0.90789795957	-2E-10
$3s$	−45.96974036708	−45.96974036910	-4E-11	$5p_{3/2}$	−0.84033954719	−0.84033954740	-3E-10
$3p_{1/2}$	−40.44829871452	−40.44829871568	-3E-11	Valence states:			
$3p_{3/2}$	−37.89430454749	−37.89430454870	-3E-11	$6s$	−0.12736806899	−0.12736806898	7E-11
$3d_{3/2}$	−28.30950025207	−28.30950025207	-1E-14	$7s$	−0.05518735931	−0.05518735931	4E-11
$3d_{5/2}$	−27.77515677536	−27.77515677489	2E-11	$6p_{1/2}$	−0.08561588462	−0.08561588462	-5E-11
$4s$	−9.51282144793	−9.51282144936	-1E-10	$7p_{1/2}$	−0.04202138669	−0.04202138668	2E-10
$4p_{1/2}$	−7.44628469483	−7.44628469556	-1E-10	$6p_{3/2}$	−0.08378548243	−0.08378548242	1E-10
$4p_{3/2}$	−6.92100118797	−6.92100118878	-1E-10	$7p_{3/2}$	−0.04136804383	−0.04136804383	5E-11

$^*\epsilon \equiv (\langle\psi|H|\psi\rangle - \varepsilon_{\rm HF})/\varepsilon_{\rm HF}$

energy and the orbital until F is properly normalised and thus an eigenstate of the Hamiltonian. This procedure is outlined in the next subsection 3.3.

Once the energy has been fine-tuned, and we have a normalised eigenstate, we continue the HF procedure. To aid convergence, however, we first "damp" the orbitals as:

$$F \to (1-\eta)F + \eta F_{\rm old}. \tag{37}$$

This both greatly increases the numerical stability, and speeds up the convergence (otherwise, orbitals tend to either oscillate between two values, or blow up). Typically, $\eta \simeq 0.5$; in the code, η is initially set to a large value (0.8), and is slowly ramped down (to 0.1) over the HF iterations (0 means no damping). So long as the equations converge, the solutions do not depend on the value chosen.

(A slightly different method for including the non-local exchange part is given in Ref. [7] on pg. 462 [also [8] pg. 495].)

3.3 Energy adjustments – finding eigenstate

Assume the correct orbital and energy can be written as $F + \delta F$, and $\varepsilon + \delta\varepsilon$, where F was the solution to Eq. (35) using the trial energy ε. Subbing this back into the HF Dirac equation, we find a new inhomogenous equation (to first order):

$$(H_{\rm HF} - \varepsilon)\delta F = \delta\varepsilon F \tag{38}$$

$$(H_{\rm l} - \varepsilon)\delta F = \delta\varepsilon F - V_{\rm nl}\delta F, \tag{39}$$

which we solve iteratively for δF and $\delta\varepsilon$. As the first step, we divide (39) by the unknown $\delta\varepsilon$, set $V_{\rm nl}\delta F = 0$, and solve for $\tilde{F} \equiv \delta F/\delta\varepsilon$ using Green's method (22). Note that we don't need to re-solve the homogeneous equation (21), since we can re-use the G_∞, G_0 solutions obtained when solving (35).

Since $(F + \delta F)$ must be normalised, we find the first guess for $\delta\varepsilon$ as (keeping only first-order terms):

$$\delta\varepsilon = \frac{\langle F|F\rangle - 1}{2\langle F|\tilde{F}\rangle}. \tag{40}$$

Then, using this $\delta\varepsilon$ and $\delta F = \delta\varepsilon\tilde{F}$, we form $V_{\rm nl}\delta F$ and solve (39) for δF. Then, we make the corrections to the orbital and energy:

$$F \to F + \delta F\,, \qquad \varepsilon \to \varepsilon + \delta\varepsilon. \tag{41}$$

This iterative procedure is continued from Eq. (39) until the energy correction drops below a specified value (i.e., until F is properly normalised). The procedure converges very rapidly, and typically is converged (for $\delta\varepsilon/\varepsilon$) to parts in 10^{20} with just two iterations.

Note that, so long as it was chosen appropriately, the non-local term $V_{\rm nl}$ is small, and so the $V_{\rm nl}\delta F$ term is even smaller and can be excluded entirely in this section without having much of an impact. Including it, however, leads to better overall convergence of the HF equations. Note that $V_{\rm nl}\delta F$ includes $V_{\rm exch}\delta F$, which must be calculated; to speed things up, we restrict this calculation to include only the $k \leq 1$ terms [see Eq. (28)], which dominate by far.

3.4 Approximate "local" exchange potential

There are several methods for obtaining a localised approximation to the HF potential, a common example is the "Hartree-Fock-Slater" method [9]. Here, I outline a slightly different method that gives reasonably good results. We use this only as a starting point for the HF/TDHF procedures, so the the final result does not depend on this potential. The choice of a good starting approximation does, however, greatly speed up the convergence of the iterative procedures.

Introducing the notation v^x_{ab} [see Eq. (27)], the non-local exchange part of the HF potential can be expressed

$$[\hat{V}_{\rm ex}F_a](r) = \sum_b v^x_{ab}(r)F_b(r). \tag{42}$$

It is non-local in that it cannot be expressed as $\hat{V}_{\rm ex}(r)\,F_a(r)$. Multiply (42) from the right and divide by $F_a^\dagger F_a$:

$$\frac{[\hat{V}_{\rm ex}F_a]F_a^\dagger}{F_a^\dagger F_a}F_a = \frac{\sum_b v^x_{ab}(r)F_b(r)F_a^\dagger(r)}{F_a^\dagger F_a}F_a(r) \tag{43}$$

$$\approx U^{(a)}_{\rm ex}(r)F_a(r). \tag{44}$$

In this way we may define $U^{(a)}_{\rm ex}(r)$, which is a localised exchange potential (for state a). Note that $U(r)$ is different for each state, and depends on the F_a orbital, and therefore must itself be found iteratively.

In theory, this is exact except for when $F_a^\dagger F_a = 0$. In practice, it is very numerically unstable whenever $F_a^\dagger F_a$ is small. However, this is not a major problem, since when F_a is small, we don't care what the exchange potential is. We proceed by introducing a cut-off, λ_a, and only calculating the exchange potential when F_a is not small. Therefore, we write

$$U^{(a)}_{\rm ex}(r) = v^x_{aa}(r) + \sum_{b\neq a} v^x_{ab}(r)\Lambda(r) \tag{45}$$

with

$$\Lambda(r) = \begin{cases} \dfrac{F_a^\dagger(r)F_b(r)}{F_a^\dagger F_a} & |F_a(r)| > \lambda_a \\ 0 & \text{otherwise} \end{cases} \tag{46}$$

Of course, we don't apply the cut-off when $b = a$ in the sum, since here the cancellation is exact and there is no numerical instability. In fact, this $a = b$ term actually gives the dominating contribution to the exchange potential. Partly, the reason this method gives such good results already is that the dominating case is treated exactly.

In the code, the cut-off is taken as

$$\lambda_a = 10^{-2}|f_a|^{\max},$$

where $|f|^{\max}$ is the maximum magnitude for the upper $f(r)$ component of F_a. Making the cut-off too small introduces numerical instabilities.

This potential leads to very good approximations for the HF orbitals and energies, and as such leads to very quick convergence of both HF and TDHF equations. For example, with normal grid choices, the energies agree with complete HF energies to five digits, and the core orbitals are orthogonal to the level of $10^{-4} - 10^{-5}$.

4 External fields

4.1 Time-dependent Hartree-Fock

In the presence of a time-varying external field with frequency ω, the orbitals will contain time-varying perturbations:

$$\psi \to \psi + \delta\psi = \psi + Xe^{-i\omega t} + Ye^{i\omega t}, \tag{47}$$

with $\varepsilon \to \varepsilon + \delta\varepsilon$. Keeping terms only to first-order, the corrections are seen to satisfy the equations (e.g., [10]):

$$\begin{aligned} (H_{HF} - \varepsilon - \omega)\, X &= -\left(\hat{h} + \delta V - \delta\varepsilon\right)\psi \\ (H_{HF} - \varepsilon + \omega)\, Y &= -\left(\hat{h}^\dagger + \delta V^\dagger - \delta\varepsilon\right)\psi, \end{aligned} \tag{48}$$

where $\hat{h}$ is the tensor operator for the external field with rank k. Here, δV is the correction to the HF potential arising due to the corrections $\{X^{(c)}, Y^{(c)}\}$ to each of the core orbitals, c.

The corrections are not (in general) states of definite angular momentum, but do have definite parity. We expand X and Y in terms of partial waves (χ and η) of definite κ (j^π):

$$\begin{aligned} X^{a,m_a} &= \sum_{\alpha,m_\alpha} X_{\alpha,m_\alpha} \\ &= \sum_{\alpha,m_\alpha} (-1)^{j_\alpha - m_\alpha} \begin{pmatrix} j_\alpha & k & j_a \\ -m_\alpha & q & m_\alpha \end{pmatrix} \chi_{\alpha,m_\alpha}. \end{aligned} \tag{49}$$

The superscript refers to the unperturbed state that X is a correction to (here $a \equiv n_a, \kappa_a$). The sum over α runs over all angular momentum states with $j_\alpha = j_a - k, ..., j_a + k$ and parity $\pi_\alpha = (-1)^{l_a + \pi}$ (where π is the parity of the operator $\hat{h}$). Note that $\{\chi_\alpha\}$ are orthogonal (and are orthogonal to ψ), and form a linearly independent set of solutions to (48).

4.2 Solving the TDHF equations

The δV term in (48) is very important and will be discussed in the next section. Here, we will ignore how it is calculated and just focus on solving the inhomogenous equations.

As before, we express the Hamiltonian as $H = H_\mathrm{l} + V_\mathrm{nl}$:

$$H_\mathrm{l} = H_0 + V_\mathrm{nuc} + V_\mathrm{dir} + U_\mathrm{x} \tag{50}$$

$$V_\mathrm{nl} = V_\mathrm{exch} - U_\mathrm{x}, \tag{51}$$

where U_x is a local approximation to the exchange potential. In the simplest case, it is $(f-1)V_\mathrm{dir}$, but better approximations aid the convergence (we use that from Sec. 3.4). It is desirable to make V_nl as small as possible.

We solve the equations iteratively, such that at the nth step:

$$\begin{aligned} &(H_l - \varepsilon \pm \omega)\, X^{(n)} = \\ &\qquad -(V_{nl}X)^{(n-1)} - \left(\hat{h} + \delta V - \delta\varepsilon^{(n-1)}\right)\psi_a, \end{aligned} \tag{52}$$

with $V_{nl}X = 0$ initially. The solution for each α is

$$X_\alpha = \frac{\phi_\alpha^\infty}{cw}\int_0^r \left\{\phi_\alpha^0|S\right\} r^2\mathrm{d}r' + \frac{\phi_\alpha^0}{cw}\int_r^\infty \left\{\phi_\alpha^\infty|S\right\} r^2\mathrm{d}r', \tag{53}$$

where the "source" term S is the rhs of Eq. (52). (Note: the $\delta\varepsilon$ term only contributes for the X term with $\alpha = a$.) The $\phi_\varkappa^{0,\infty}$ functions here are the solutions with Dirac quantum number α to the homogenous equation (21), including both the angular part and the $1/r$. We defined here the "partial" matrix elements, that include only the integral over angular coordinates:

$$\left\{\psi_a|\hat{h}|\psi_b\right\} \equiv \int \psi_a^\dagger \hat{h}\psi_b\,\mathrm{d}\Omega. \tag{54}$$

We similarly define the partial reduced matrix element:

$$\left\{\psi_a|T_q^k|\psi_b\right\} \equiv (-1)^{j_a - m_a}\begin{pmatrix} j_a & k & j_b \\ -m_a & q & m_b \end{pmatrix}\left\{\psi_a||T^k||\psi_b\right\}. \tag{55}$$

Then, in terms of the partial waves (χ), the solution becomes:

$$\chi_\alpha = \frac{\phi_\alpha^\infty}{cw}\int_0^r \left\{\phi_\alpha^0||S\right\} r^2\mathrm{d}r' + \frac{\phi_\alpha^0}{cw}\int_r^\infty \left\{\phi_\alpha^\infty||S\right\} r^2\mathrm{d}r'. \tag{56}$$

This is done so that one needs only to calculate the (m-independent) reduced matrix element of $\hat{h}$. The radial integral $|\chi_\alpha|^2$ is used to control convergence here (for including the non-local exchange part). Using U_x from Sec. 3.4, convergence (for a given orbital) to parts in 10^9 is typically reached in ~ 10 iterations.

From perturbation theory, the correction (excluding δV and considering the case with $\delta\varepsilon = 0$) can also be expressed as:

$$|X\rangle = \sum_n \frac{|n\rangle\langle n|\hat{h}|\psi\rangle}{\varepsilon - \varepsilon_n + \omega}, \tag{57}$$

which can be used to test the method. Consider, e.g., the matrix element:

$$\langle m|X\rangle = \frac{\langle m|\hat{h}|\psi\rangle}{\varepsilon - \varepsilon_m + \omega}, \tag{58}$$

$$\langle m|\chi\rangle = \frac{\langle m||\hat{h}||\psi\rangle}{\varepsilon - \varepsilon_m + \omega}, \tag{59}$$

which can be calculated both ways (lhs vs rhs); see Table 2.

An important application of this technique is that it allows calculations to be done without requiring a summation over the complete set of intermediate states (replaced by solving the inhomogeneous differential equation). This method of

Table 2: Testing TDHF method using Eq. (59) for Cs, with $m = 6p_{1/2}$, $\psi = 6s_{1/2}$ (Hartree-Fock level, no δV).

Operator	(59) lhs	(59) rhs	ϵ^*
$h_{\rm E1}$ $(\omega = \omega_{\rm HF})$	63.2029312	63.2025676	6×10^{-6}
$h_{\rm E1}$ $(\omega = 0)$	126.405501	126.405135	3×10^{-6}
$h_{\rm PNC}$ $(\omega = 0)$	-1.0700928	-1.0700932	4×10^{-7}

$^*\epsilon \equiv (lhs - rhs)/lhs$

performing exact summation over intermediate states is sometimes called the Solving Equations, Mixed States, or Dalgarno-Lewis method [11], depending on context. In this example (59) the intermediate-states summation is trivial, since it involves only single operator and hence only a single intermediate state contributes. In general, all intermediate states (including continuum and positive energy states) contribute, so this method allows calculations without the need for a large basis. See also Sec. 5.1 below for a test of the Dalgarno-Lewis method for calculating PNC amplitudes.

4.3 Core polarisation (RPA)

This section largely follows Ref. [10] (see also [12–15]). In the presence of an external field, the core electrons become perturbed and a correction to the HF potential is induced. This effect is often called the core polarisation, and is particularly important, since it involves corrections with single excitations from the HF core (in the absence of an external field, the lowest-order corrections to the HF potential involve two excitations). The method described here is equivalent to and is often referred to as the random phase approximation (RPA).

To account for core polarisation, the set of TDHF equations (48) are solved self-consistently for each of the core orbitals using the method from Sec. 4.1. The δV term is the correction to the HF potential:

$$\delta V = V_{\rm HF}(\{\psi_b + \delta\psi^b\}) - V_{\rm HF}(\{\psi_b\}), \tag{60}$$

where $\{\psi_b\}$ denotes the set of all core orbitals, and the single-particle energy correction is

$$\delta\varepsilon = \langle\psi_b|\hat{h} + \delta V|\psi_b\rangle. \tag{61}$$

The TDHF equations are solved iteratively, updating the δV and $\delta\varepsilon$ terms at each step until convergence is reached; i.e., at the nth step, we have

$$(H_{HF} - \varepsilon - \omega)\, X_\beta^{(n)} = -\left(\hat{h} + \delta V^{(n-1)} - \delta\varepsilon^{(n-1)}\right)\psi_b, \tag{62}$$

with $\delta V = 0$ for the initial iteration (similar for Y). After integrating over angles, the $\delta\varepsilon$ term only appears in the equations when $\beta = b$, which for odd-parity operators is never the case.

Combining Eqs. (60) with (26), we have:

$$\begin{aligned}\delta V\phi_a(\boldsymbol{r}_1) = \sum_{i\neq a}^{N_c}\Bigg(&\int\frac{\phi_i^\dagger(\boldsymbol{r}_2)X^i(\boldsymbol{r}_2)}{|\boldsymbol{r}_{12}|}{\rm d}^3\boldsymbol{r}_2\,\phi_a(\boldsymbol{r}_1)\\ &+\int\frac{Y^{i\dagger}(\boldsymbol{r}_2)\phi_i(\boldsymbol{r}_2)}{|\boldsymbol{r}_{12}|}{\rm d}^3\boldsymbol{r}_2\,\phi_a(\boldsymbol{r}_1)\\ &-\int\frac{\phi_i^\dagger(\boldsymbol{r}_2)\phi_a(\boldsymbol{r}_2)}{|\boldsymbol{r}_{12}|}{\rm d}^3\boldsymbol{r}_2\,X^i(\boldsymbol{r}_1)\\ &-\int\frac{Y^{i\dagger}(\boldsymbol{r}_2)\phi_a(\boldsymbol{r}_2)}{|\boldsymbol{r}_{12}|}{\rm d}^3\boldsymbol{r}_2\,\phi_i(\boldsymbol{r}_1)\Bigg),\end{aligned} \tag{63}$$

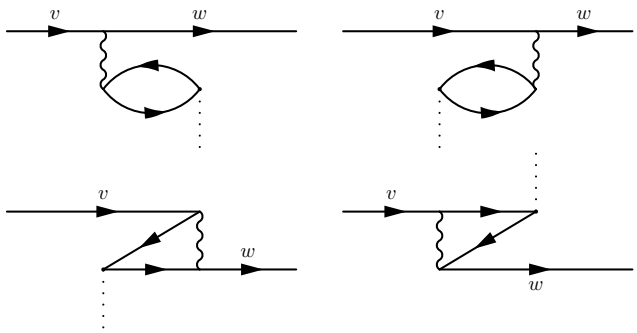

Figure 4: Diagrams representing the lowest order direct and exchange core-polarisation (RPA) corrections to the $\langle w|\hat{h}|v\rangle$ amplitude. Wavy line is Columb interaction, dotted line is external field ($\hat{h}$). All internal lines are summed over: forwards lines are virtual excited states, backward lines are holes in the core. In higher-order diagrams, each $\hat{h}$ vertex is corrected again (RPA).

using notation of Eq. (49). The reduced matrix elements are:

$$\begin{aligned}\langle\phi_n||\delta V||\phi_a\rangle = \sum_{b\beta}\Bigg(&\frac{C^k_{na}C^k_{\beta b}}{[k]}(R^k_{nba\beta} + R^k_{nba\beta'})\\ &-(-1)^{j_\beta - j_a}\sum_\lambda(-1)^{k+\lambda}\Bigg[C^\lambda_{ab}C^\lambda_{n\beta}\begin{Bmatrix}j_a & j_n & k\\ j_\beta & j_b & \lambda\end{Bmatrix}R^\lambda_{na\beta b}\\ &+C^\lambda_{a\beta}C^\lambda_{nb}\begin{Bmatrix}j_a & j_n & k\\ j_b & j_\beta & \lambda\end{Bmatrix}R^\lambda_{nab\beta'}\Bigg]\Bigg),\end{aligned} \tag{64}$$

where the sum b runs over all core orbitals, and β runs over all (partial wave) corrections to b. The prime (β') means the η_β orbital is used; no prime means χ_β. The equation for $\langle\phi_n||\delta V^\dagger||\phi_a\rangle$ is the same, but with $\beta \leftrightarrow \beta'$. For the "partial" reduced matrix elements [see Eqs. (56), (55)], make substitution: $R^k_{abcd} \to y^k_{bd}F_c$. Here, C^k_{ab} is given by Eq. (30),

$$R^k_{abcd} \equiv \int{\rm d}r_1\,\left[f_a(r_1)f_c(r_1) + g_a(r_1)g_c(r_1)\right]\,y^k_{bd}(r_1), \tag{65}$$

and y^k_{bd} is given by Eq. (29).

In this method, matrix elements of the operator $\hat{h}$ between valence states v and w are calculated, including the effect of core polarisation (i.e., including the effect of $\hat{h}$ operating on the core electrons) as [10]

$$\langle w|\hat{h} + \delta V|v\rangle, \tag{66}$$

which is equivalent to the RPA method (see, e.g., Ref. [3]). If the equations (62) are solved just once, without further iterations, this corresponds to the lowest (first) order corrections to the amplitude, which are shown diagramatically in Fig. 4. Further iterations correspond to higher-orders. Once the equations have converged, the core polarisation is taken into account to all-orders.

Core polarisation can by included into the Dalgarno-Lewis method for exact summation over intermediate states by solving the equation (48) for the required valence states (including the δV, which must be found first).

4.3.1 Algebraic method

The THDF equations can also be solved using an algebraic method, by expanding the χ and η corrections over a basis of

states (method for constructing such a basis will be discussed in the next section):

$$\chi^{\varkappa} = \sum_j a_j x_j\,, \qquad \eta^{\varkappa} = \sum_j b_j x_j\,, \tag{67}$$

where $\{x_j\}$ is the set of basis orbitals, and $\{a_j/b_j\}$ are the expansion coefficients. Multiply Eq. (48) from the left by $x_i^\dagger$ (and integrate), which yields the matrix equations:

$$\begin{aligned}[H_{ij} - (\varepsilon-\omega)S_{ij}]\,a_j &= -h_{ic} - \delta V_{ic} + \delta\varepsilon_c S_{ic}\delta_{\kappa_i\kappa_c}\\ [H_{ij} - (\varepsilon+\omega)S_{ij}]\,b_j &= -h^\dagger_{ic} - \delta V^\dagger_{ic} + \delta\varepsilon_c S_{ic}\delta_{\kappa_i\kappa_c}.\end{aligned} \tag{68}$$

Here

$$\begin{aligned}H_{ij} &= \langle x_i|\hat{H}_{\rm HF}|x_j\rangle\,, \qquad S_{ij} = \langle x_i|x_j\rangle\,,\\ h_{ic} &= \langle x_i||\hat{h}||\psi_c\rangle\,, \qquad \delta\varepsilon_c = \langle\psi_c||\hat{h}+\delta V||\psi_c\rangle,\end{aligned} \tag{69}$$

δV_{ic} is given by Eq. (64), and the delta function means the $\delta\varepsilon$ term only appears for partial-wave corrections with $\kappa = \kappa_c$.

There are two ways to proceed. The simplest way is to solve (68), which is a pair of linear matrix equations, for the set of expansion coefficients, a_j and b_j. This must be solved for each partial wave correction ($\varkappa_i$) to each core state c. Note, however, that δV depends on the corrected states, and thus on a and b; so this would have to be solved iteratively. In another approach, the δV term is also expanded in terms of the basis; then no iterations are required, and the equations take the form of a generalised eigenvalue problem, see Ref. [15].

4.4 Core polarisation (diagram technique, RPA)

[This is not yet tested or fully implemented in the code]

The core polarisation correction to a matrix element can also be taken into account by directly evaluating the four diagrams in Fig. 4. If, to lowest order, the matrix element of operator $\hat{h}$ is $h^{(0)}_{ij}$, including the first-order correction it becomes [2]

$$h_{ij} = h^{(0)}_{ij} + \delta h_{ij} \tag{70}$$

$$\delta h_{ij} = \sum_{ma}\frac{h^{(0)}_{am}\tilde{g}_{imja}}{\varepsilon_a-\varepsilon_m-\omega} + \sum_{ma}\frac{h^{(0)}_{ma}\tilde{g}_{iajm}}{\varepsilon_a-\varepsilon_m+\omega}, \tag{71}$$

where $\tilde{g}_{abcd} = g_{abcd} - g_{abdc}$ is the symmetrised Coulomb integral, with

$$g_{abcd} = \sum_{kq}(-1)^q\langle\kappa_a m_a|C^k_{-q}|\kappa_c m_c\rangle\langle\kappa_b m_b|C^k_q|\kappa_d m_d\rangle R^k_{abcd}. \tag{72}$$

The a sum runs over all occupied core electrons, while m runs over all virtual excited states.

In the RPA method, the lowest-order matrix elements in δh_{ij} are then replaced with the corrected values. This process is repeated iteratively (for all core states i and j) until convergence is reached; i.e., at the nth iteration we have:

$$\delta h^n_{ij} = \sum_{ma}\frac{(h^{(0)}_{am}+\delta h^{n-1}_{am})\tilde{g}_{imja}}{\varepsilon_a-\varepsilon_m-\omega} + \sum_{ma}\frac{(h^{(0)}_{ma}+\delta h^{n-1}_{ma})\tilde{g}_{iajm}}{\varepsilon_a-\varepsilon_m+\omega}. \tag{73}$$

Then, in terms of reduced matrix elements, the RPA matrix element is:

$$\langle i||h||j\rangle^{\rm RPA} = \langle i||h||j\rangle + \langle i||\delta h||j\rangle \tag{74}$$

with

$$\langle i||\delta h||j\rangle = \frac{1}{[k]}\sum_{am}(-1)^{j_a-j_m+k}\left(\frac{\langle a||t||m\rangle^{\rm RPA}Z^k_{imja}}{\varepsilon_a-\varepsilon_m-\omega} + \frac{\langle m||t||a\rangle^{\rm RPA}Z^k_{iajm}}{\varepsilon_a-\varepsilon_m+\omega}\right), \tag{75}$$

where

$$Z^k_{abcd} \equiv (-1)^{j_a+j_b+1}\left(Q^k_{abcd} + \sum_\lambda[k]\begin{Bmatrix} j_c & j_a & k\\ j_d & j_b & \lambda\end{Bmatrix}Q^\lambda_{abdc}\right). \tag{76}$$

These expressions have been taken from Ref. [3]. RPA matrix elements between valence states have the same expression (the equations need only be iterated for the core electrons).

5 Finite basis of orbitals

In many problems in perturbation theory, a summation over the full (infinite) set of orbitals is required. In theory, a basis of HF orbitals can be used for this. However, such a basis generally converges very slowly, requires a very large radial grid, and the solutions become numerically unstable for low energies. Further, sum over all states must include the integral over all positive- and negative-energy continuum states, which can be a significant contribution. Instead, it is common to introduce a finite basis for the radial Dirac equation, see, e.g., Ref. [16]. We assert that all orbitals go to zero at the boundary of a subset of the radial grid, $r_{\rm max}$. This is equivalent to placing the atom in the centre of an infinite spherical "square-well" potential. In this case, a complete set of orbitals can be approximately expanded in terms of a finite number of states, which includes the $\varepsilon > 0$ continuum states. So long as the size of the cavity is large compared to typical radius of orbitals we are directly interested in, the results should be independent of the cavity size.

5.1 B-spline basis

The spectrum of orbitals to be used in the calculations are expanded as

$$F_{n\kappa} = \sum_i^{2N} p_i S_i(r), \tag{77}$$

where $\{S_i\}$ are a set of $2N$ basis orbitals that form a complete set over a sub-domain of the radial grid $[0, r_{\rm max}]$ (N is defined this way because of the duel set of positive/negative energy solutions to the Dirac equation). The $\{p_i\}$ expansion coefficients are found diagonalising the set of basis orbitals with respect to the Hamiltonian matrix. In practise, this is done by solving the eigenvalue problem:

$$H_{ij}p_i = \varepsilon S_{ij}p_i, \tag{78}$$

with

$$H_{ij} = \langle S_i|\hat{H}_{\rm HF}|S_j\rangle\,, \qquad S_{ij} = \langle S_i|S_j\rangle. \tag{79}$$

There are $2N$ solutions of eigenvalues ε with corresponding eigenvectors $\vec{p}$, which correspond to the spectrum of stationary states; N of these correspond to negative-energy ($\varepsilon < -mc^2$) states. If the S set is orthonormal, B is just the identity, but in general it is not. Note that A and B are positive-definite real

Table 3: Comparison between energies of spline (DKB) basis orbitals and finite-difference Hartree Fock orbitals. The basis was constructed using 50 B-splines of order 7 in a cavity of radius $30\,a_B$ with the first internal point at $r = 10^{-5}\,a_B$ (only the first 10 splines of each symmetry are shown). Final column shows the root-mean-square radii for the Hartree Fock orbitals. The spline basis energies agree very well (better than parts in 10^6) with the Hartree Fock energies, so long as the cavity is large compared to the typical radius of the orbital in question; for higher orbitals, where this is not the case, the energies diverge significantly. [$\epsilon = (A-B)/A$]

	$s_{1/2}$				$p_{1/2}$			
n	$\varepsilon_{\rm spline}$	$\varepsilon_{\rm HF}$	ϵ	$\langle r^2\rangle^{1/2}_{\rm HF}$	$\varepsilon_{\rm spline}$	$\varepsilon_{\rm HF}$	ϵ	$\langle r^2\rangle^{1/2}_{\rm HF}$
1	−1330.1186542	−1330.1188558	−2e−7	0.03				
2	−212.5644469	−212.5644963	−2e−7	0.12	−199.4294948	−199.4295038	−5e−8	0.10
3	−45.9697097	−45.9697486	−8e−7	0.32	−40.4482937	−40.4483086	−4e−7	0.31
4	−9.5127994	−9.5128206	−2e−6	0.74	−7.4462753	−7.4462846	−1e−6	0.77
5	−1.4898011	−1.4898044	−2e−6	1.88	−0.9078963	−0.9078975	−1e−6	2.15
6	−0.1273679	−0.1273681	−1e−6	6.52	−0.0856153	−0.0856159	−6e−6	8.65
7	−0.055047	−0.0551874	−3e−3	14.58	−0.0411125	−0.0420214	−2e−2	18.16
8	−0.0240059	−0.0309525	−3e−1	25.77	−0.0110954	−0.0251205	−8e−1	30.79
9	0.0147887	−0.0198146		40.11	0.0314743	−0.0167280		46.56
10	0.0679063	−0.0137713		57.61	0.0877553	−0.0119427		65.48

matrices. States of different κ are orthogonal, so the A matrix can be chosen to be block diagonal, meaning the eigenvalue problem can solved separately for each block (each κ); i.e. the expansion is performed separately for each κ using the same underlying basis functions.

The choice of basis must account for the boundary conditions for the stationary states. A good choice of basis allows for convergence of many-body problems with fewer basis states. The particular choice we use is called the Duel-Kinetic-Balance (DKB) B-spline basis as introduced in Ref. [17];

$$S_i^{\rm DKB} = \begin{cases} \begin{pmatrix} b_i(r) \\ \frac{\alpha}{2}\left(\partial_r + \kappa/r\right) b_i(r) \end{pmatrix} & 0 \le i < N \\ \begin{pmatrix} \frac{\alpha}{2}\left(\partial_r - \kappa/r\right) b_{i-N}(r) \\ b_{i-N}(r) \end{pmatrix} & N \le i < 2N. \end{cases} \tag{80}$$

full details, including on including boundary conditions, are given in that work (see also [16, 18]). Note that the boundary conditions are met by discarding some of the underlying b-splines; when we talk of an expansion using N splines, we refer only to the ones that are kept; the underlying spline basis consists of a slightly larger set [17]. Another common choice, which we refer to as the Notre-Dame (ND) basis [16] may be formed with the lower-component of (80) set to zero for $i < N$, and the upper set to zero for $i \ge N$; this set requires extra conditions for the boundary conditions to be met [16].

Each B-spline, $b_i^{(k)}(r)$, is a polynomial of degree $k-1$, that is non-zero only inside the interval $t_i \le r < t_{i+k}$, where $\{t_i\}$ are a set of $(N+k-2)$ "knots" (the S_i basis orbitals are non-zero also only in this region). The first interior knot is placed at r_0 (with one also defined at $r = 0$), the last at $r_{\rm max}$, and the rest are distributed uniformly along the u radial grid (if we are using a logarithmic grid, they will distributed exponentially along r, see Sec. 2.2). The piecewise nature of the splines simplifies the evaluation of integrals, and acts to make the A and S matrices banded, which can typically be solved with high numerical precision.

The first interior knot is placed at r_0, and the last at $r_{\rm max}$; the basis orbitals are defined only inside this region (and are zero outside). By default, this is the same as the total radial grid, but the basis orbitals are typically defined on a smaller sub-domain. The benefit of restricting the radial sub-domain for the basis is that reasonable completeness can be achieved with fewer basis functions. However, increasing r_0 too much loses the low-r behaviour of the basis orbitals, and making $r_{\rm max}$ too small loses the correspondence between the "real" and basis orbitals. The ideal choice of sub-domain depends on the specifics of the problem.

Table 3 shows the energies of spline orbitals, using 50 B-splines of order 7 in a cavity of radius $30\,a_B$ with the first internal point at $r = 10^{-5}\,a_B$. This spline basis is orthogonal (or normal) with respect to the Hartree-Fock core to parts in 10^6; the basis itself is orthogonal to parts in 10^{15}. Table 4 shows hyperfine constants calculated using spline orbitals, which is a test of the low-r performance of the orbitals.

One way to test the basis is to consider the parity non-conservation (PNC) amplitude, which is a correction to the (otherwise forbidden) $E1$ transition between states of the same parity, due to the parity-violating weak interaction between the electrons and nucleus (see, e.g., Ref. [19]). This can be expressed as a sum over intermediate states n:

$$E^{(z)}_{\rm PNC} = \frac{\langle B|\boldsymbol{d}_z|n\rangle\langle n|h_{\rm W}|A\rangle}{\varepsilon_A - \varepsilon_n} + \frac{\langle B|h_{\rm W}|n\rangle\langle n|\boldsymbol{d}_z|A\rangle}{\varepsilon_B - \varepsilon_n} \tag{81}$$

where $\boldsymbol{d}$ is the $E1$ operator, and $h_{\rm W}$ is the PNC operator. Using the TDHF (Dalgarno-Lewis) method as described in Sec. 4.1, this can also be expressed in two other formally equivalent ways:

$$E^{(z)}_{\rm PNC} = \langle B|\boldsymbol{d}_z|\delta A^{(W)}\rangle + \langle \delta B^{(W)}|\boldsymbol{d}_z|A\rangle \tag{82}$$

$$= \langle \delta B^{(d)}|h_{\rm W}|A\rangle + \langle B|h_{\rm W}|\delta A^{(d)}\rangle, \tag{83}$$

(which we refer to here as the δW and δd method, respectively), where $\delta A^{(W/d)}$ is the correction to orbital A due to the weak/E1 interaction. Comparing the results of Eqs. (82) and (83) tests the numerical accuracy of the Dalgarno Lewis (solving-equations) method, and comparing these to the result of (81) gives a good test of the basis. The two forms of the Dalgarno Lewis method agree to parts in 10^8. Comparison between the PNC amplitude as calculated using this and the direct-summation method is in Table 5.

6 Radiative QED corrections

Radiative QED corrections can be included into the wavefunctions using the radiative potential method developed in Ref. [20], including the (small) finite nuclear size corrections [21, 22]. In this method, an effective potential, $V_{\rm rad}$,

Table 4: Magnetic dipole hyperfine constants A (assuming a point-like nuclear magnetisation distribution), as calculated using the finite-difference Hartree-Fock orbitals, and the DKB basis constructed using 50 B-splines of order 7 in a cavity of radius $50\,a_B$, with varying first internal point (A is sensitive to orbitals at small radial distances). [$\epsilon = (A-B)/A$]

		$r_0 = 10^{-4}\,a_B$		$10^{-5}\,a_B$		$10^{-6}\,a_B$	
n	$A_{\rm HF}$	$A_{\rm Spline}$,	ϵ	$A_{\rm Spline}$,	ϵ	$A_{\rm Spline}$,	ϵ
1	3.9180×10^{7}	3.8361×10^{7}	-2×10^{-2}	3.9172×10^{7}	-2×10^{-4}	3.9179×10^{7}	-3×10^{-6}
2	4.6208×10^{6}	4.5209×10^{6}	-2×10^{-2}	4.6199×10^{6}	-2×10^{-4}	4.6207×10^{6}	-3×10^{-6}
3	9.3463×10^{5}	9.1437×10^{5}	-2×10^{-2}	9.3446×10^{5}	-2×10^{-4}	9.3462×10^{5}	-1×10^{-5}
4	1.9822×10^{5}	1.9392×10^{5}	-2×10^{-2}	1.9819×10^{5}	-2×10^{-4}	1.9823×10^{5}	4×10^{-5}
5	2.7987×10^{4}	2.7380×10^{4}	-2×10^{-2}	2.7982×10^{4}	-2×10^{-4}	2.7988×10^{4}	5×10^{-5}
6	1.4337×10^{3}	1.4022×10^{3}	-2×10^{-2}	1.4334×10^{3}	-2×10^{-4}	1.4336×10^{3}	-4×10^{-5}
7	3.9394×10^{2}	3.8532×10^{2}	-2×10^{-2}	3.9386×10^{2}	-2×10^{-4}	3.9394×10^{2}	-2×10^{-5}
8	1.6448×10^{2}	1.6397×10^{2}	-3×10^{-3}	1.6760×10^{2}	2×10^{-2}	1.6763×10^{2}	2×10^{-2}

Table 5: Comparison of PNC amplitudes (at the HF level) for ^{133}Cs as calculated using the Dalgarno-Lewis (DL) method, and direct summation using a spline basis [formed in a cavity of $(10^{-6}, 50)\,a_B$ using N splines of order k].

		Direct Summation: N/k		
Transition	DL	50/5	60/6	70/7
$6s-7s$	-0.73954	-0.73948	-0.73953	-0.73954
$6s-5d_{3/2}$	-2.4000	-2.3998	-2.4000	-2.4000

is added to the Hamiltonian before the equations are solved. The potential can be written as the sum of the Uehling (vacuum polarisation) and self-energy potentials. The self-energy potential itself is written as the sum of the high- and low-frequency electric contributions, and the magnetic contribution:

$$V_{\rm rad}(\boldsymbol{r}) = V_{\rm Ueh}(r) + V^{h}_{\rm SE}(r) + V^{l}_{\rm SE}(r) + V^{\rm mag}_{\rm SE}(\boldsymbol{r}). \qquad (84)$$

The inclusion of this potential into the Hartree-Fock equations (instead of adding it as a perturbation after HF has converged) gives an important contribution (core relaxation), especially for states with $l > 0$. The first three (electric) terms on the RHS of Eq. (84) ,

$$H^{\rm el}(r) = V_{\rm Ueh}(r) + V^{h}_{\rm SE}(r) + V^{l}_{\rm SE}(r),$$

are simple scalar terms, and can be included into the calculations simply (e.g., by adding them to the nuclear potential). The final (magnetic) term, which can be expressed as [22]

$$V^{\rm mag}_{\rm SE}(\boldsymbol{r}) = i(\boldsymbol{\gamma}\cdot\boldsymbol{n})H^{\rm mag}(r), \qquad (85)$$

leads to off-diagonal terms in the Hamiltonian. Together, they can be included by making additions to the radial derivative [see Eq. (15)]:

$$\partial_r F = \frac{1}{c}\begin{pmatrix} c(-\kappa/r + H^{\rm mag}) & (\varepsilon - \hat{V} + H^{\rm el} + 2c^2) \\ -(\varepsilon - \hat{V} + H^{\rm el}) & c(\kappa/r - H^{\rm mag}) \end{pmatrix} F. \qquad (86)$$

The sign convention here for $V_{\rm rad}$ (i.e., with $\hat{H} \to \hat{H} - V_{\rm rad}$) is from Ref. [20].

Detailed expressions for the individual contributions to $V_{\rm rad}$ are given in Refs. [20–22] – they involve some rather nasty integrals that must be evaluated carefully.[8] Note that, due to the presence of double integrals, the high-frequency term $V^{hf}_{\rm SE}$ is quite expensive to calculate. To speed this up, we calculate it only every $n \approx 5$ points along the grid and use cubic interpolation for the intermediate points.

[8] Note: there is a small typo in Eq. (14) of Ref. [22] ($V^{\rm step}_{\rm high}$); the $r \le r_N$ and $r > r_N$ terms should be swapped.

Appendix

Some useful equations, definitions are given; see, e.g., [3, 23–26]. Note that I have introduced some notation not found in the above sources, and some of the notation differs between sources.

A Coulomb Integrals

The Coulomb integral g_{abcd} can be expressed:

$$\begin{aligned} g_{abcd} &\equiv \int \mathrm{d}r_1^3 \mathrm{d}r_2^3\, \psi_a^\dagger(\boldsymbol{r_1})\psi_b^\dagger(\boldsymbol{r_2})\frac{1}{|\boldsymbol{r}_{12}|}\psi_c(\boldsymbol{r_1})\psi_d(\boldsymbol{r_2}) \\ &= \sum_{kq}(-1)^q\langle\kappa_a m_a|C^k_{-q}|\kappa_c m_c\rangle\langle\kappa_b m_b|C^k_q|\kappa_d m_d\rangle R^k_{abcd}, \end{aligned} \tag{87}$$

where we used the Laplace expansion:

$$\frac{1}{r_{12}} = \sum_{kq}\frac{r^k_<}{r^{k+1}_>}(-1)^q C^k_{-q}(\boldsymbol{n}_1)C^k_q(\boldsymbol{n}_2), \tag{88}$$

with $r_< = \min(r, r')$, and

$$C^k_q \equiv \sqrt{\frac{4\pi}{2k+1}}Y_{kq}(\boldsymbol{n}). \tag{89}$$

$$\sum_{m_b} g_{abab} = [j_b]R^0_{abab}. \tag{90}$$

The R^k_{abcd} factor is defined as:

$$R^k_{abcd} = \int \mathrm{d}r_1\ \left[f_a(r_1)f_c(r_1) + g_a(r_1)g_c(r_1)\right]\, y^k_{bd}(r_1) \tag{91}$$

which has symmetry: $c \leftrightarrow a,\ b \leftrightarrow d,\ (ac) \leftrightarrow (bd)$:

$$\begin{aligned} R^k_{abcd} = R^k_{cbad} = R^k_{adcb} = R^k_{cdab} \\ = R^k_{badc} = R^k_{bcda} = R^k_{dabc} = R^k_{dcba}, \end{aligned} \tag{92}$$

and the symmetric $y^k_{bd}(r) = y^k_{db}(r)$ integral is defined:

$$y^k_{bd}(r) = \int_0^\infty \frac{r^k_<}{r^{k+1}_>}\left[f_a f_b + g_a g_b\right](r')\,\mathrm{d}r'. \tag{93}$$

Note that:

$$\langle\kappa_a||C^k||\kappa_b\rangle \equiv C^k_{ab} \equiv (-1)^{j_a+1/2}\widetilde{C}^k_{ab}, \tag{94}$$

$$= (-1)^{j_a+1/2}\sqrt{[j_a][j_b]}\begin{pmatrix} j_a & j_b & k \\ -1/2 & 1/2 & 0\end{pmatrix}\pi(l_a, l_b, k) \tag{95}$$

where $\widetilde{C}^k_{ac}$ is a short-hand notation that is useful since $\widetilde{C}^k_{ac} = \widetilde{C}^k_{ca}$.

We further define the useful integrals:

$$\begin{aligned} X^k_{abcd} &\equiv (-1)^k\langle\kappa_a||C^k||\kappa_c\rangle\langle\kappa_b||C^k||\kappa_d\rangle R^k_{abcd} \\ &= (-1)^{j_a+j_b+1}Q^k_{abcd}, \end{aligned} \tag{96}$$

$$Q^k_{abcd} = (-1)^k\widetilde{C}^k_{ac}\widetilde{C}^k_{bd}R^k_{abcd} \tag{97}$$

and

$$\begin{aligned} Z^k_{abcd} &\equiv X^k_{abcd} + \sum_\lambda [k]\begin{Bmatrix} j_c & j_a & k \\ j_d & j_b & \lambda\end{Bmatrix}X^\lambda_{abdc} \\ &= (-1)^{j_a+j_b+1}\left(Q^k_{abcd} + \sum_\lambda [k]\begin{Bmatrix} j_c & j_a & k \\ j_d & j_b & \lambda\end{Bmatrix}Q^\lambda_{abdc}\right). \end{aligned} \tag{98}$$

Here Q^k_{abcd} is convenient due to the symmetries $c \leftrightarrow a,\ b \leftrightarrow d,\ (ac) \leftrightarrow (bd)$:

$$\begin{aligned} Q^k_{abcd} = Q^k_{cbad} = Q^k_{adcb} = Q^k_{cdab} \\ = Q^k_{badc} = Q^k_{bcda} = Q^k_{dabc} = Q^k_{dcba}. \end{aligned} \tag{99}$$

B Angular integrals + identities

Wigner-Eckhardt theorem

See, e.g., Refs. [24, 25]:

$$\begin{aligned} &\langle n_a\kappa_a m_a|T^k_q|n_b\kappa_b m_b\rangle \\ &\quad = (-1)^{j_a-m_a}\begin{pmatrix} j_a & k & j_b \\ -m_a & q & m_b\end{pmatrix}\langle n_a\kappa_a||T^k||n_b\kappa_b\rangle \end{aligned} \tag{100}$$

$$\langle j||T^k||j'\rangle = (-1)^{j-j'}\langle j'||T^k||j\rangle^* \tag{101}$$

$$\begin{aligned} &\langle J'IF'||T^k||JIF\rangle \\ &\quad = (-1)^{F+J'+I+k}\sqrt{[F'][F]}\begin{Bmatrix} J & I & F \\ F' & k & J'\end{Bmatrix}\langle J'||T^k||J\rangle \end{aligned} \tag{102}$$

where $([a] \equiv 2a+1)$.

$$\sum_{m_a,m_b,q}|\langle n_a\kappa_a m_a|T^k_q|n_b\kappa_b m_b\rangle|^2 = |\langle n_a\kappa_a||T^k||n_b\kappa_b\rangle|^2. \tag{103}$$

Clebsch-Gordon coefficients notation

$$\langle j_1 m_1, j_2 m_2|JM\rangle \equiv (-1)^{j_1-j_2+M}\sqrt{[J]}\begin{pmatrix} j_1 & j_2 & J \\ m_1 & m_2 & -M\end{pmatrix} \tag{104}$$

$$\equiv C(j_1, j_2, J; m_1, m_2, M) \tag{105}$$

$$\equiv C^{JM}_{j_1 m_1, j_2 m_2}. \tag{106}$$

$$|j_1 j_2; JM\rangle = \sum_{m_1,m_2}\langle j_1 m_1, j_2 m_2|JM\rangle|j_1 m_1\rangle|j_2 m_2\rangle \tag{107}$$

Some angular integrals + matrix elements

$$\begin{aligned} &\int Y_{l'm'}Y_{lm}Y_{LM}\,\mathrm{d}\Omega \\ &\quad = \sqrt{\frac{[l'][l][L]}{4\pi}}\begin{pmatrix} l' & l & L \\ 0 & 0 & 0\end{pmatrix}\begin{pmatrix} l' & l & L \\ m' & m & M\end{pmatrix} \end{aligned} \tag{108}$$

$$\sum_{jm}(2j+1)\begin{pmatrix} j_1 & j_2 & j \\ m_1 & m_2 & m\end{pmatrix}\begin{pmatrix} j_1 & j_2 & j \\ m_1' & m_2' & m\end{pmatrix} = \delta_{m_1 m_1'}\delta_{m_2 m_2'} \tag{109}$$

$$\sum_{m_1 m_2}(2j+1)\begin{pmatrix} j_1 & j_2 & j \\ m_1 & m_2 & m\end{pmatrix}\begin{pmatrix} j_1 & j_2 & j' \\ m_1 & m_2 & m'\end{pmatrix} = \delta_{jj'}\delta_{mm'} \tag{110}$$

$$\sum_{m_l=-l}^{l}|Y_{lm_l}|^2 = \frac{2l+1}{4\pi} \tag{111}$$

$$\sum_m |\Omega_{\kappa m}|^2 = \frac{2j+1}{4\pi} \tag{112}$$

$$\begin{aligned} &\langle\kappa_a||C^k||\kappa_b\rangle \\ &\quad = (-1)^{j_a+1/2}\sqrt{[j_a][j_b]}\begin{pmatrix} j_a & j_b & k \\ -1/2 & 1/2 & 0\end{pmatrix}\pi(l_a+l_b+k) \end{aligned} \tag{113}$$

$\pi(x) = 1$ if x is even, but $= 0$ if x is odd.

$$\langle l_a||C^k||l_b\rangle = (-1)^{l_a}\sqrt{[l_a][l_b]}\begin{pmatrix} l_a & l_b & k \\ 0 & 0 & 0\end{pmatrix} \tag{114}$$

$$\langle n\kappa||r_z||n'\kappa'\rangle = (n\kappa|r|n'\kappa')\langle\kappa||C^1||\kappa'\rangle \tag{115}$$

From Ch. 13 of Ref. [25]:

$$\begin{aligned} &\langle jls||l||j'l's'\rangle \\ &\quad = \delta_{ll'}\delta_{ss'}(-1)^{j'+l+s+1}\sqrt{[j][j'][l]l(l+1)}\begin{Bmatrix} j & 1 & j' \\ l & s & l\end{Bmatrix} \end{aligned} \tag{116}$$

$$\langle jls||s||j'l's'\rangle = \delta_{ll'}\delta_{ss'}(-1)^{j+l+s+1}\sqrt{[j][j'][s]s(s+1)}\begin{Bmatrix} j & 1 & j' \\ s & l & s \end{Bmatrix} \quad (117)$$

C Useful definitions/identities

Dirac matrices

Dirac matrices are defined by the relation:

$$\{\gamma^\mu, \gamma^\nu\} = 2g^{\mu\nu}, \quad (118)$$

and have the properties:

$$\gamma^i\gamma^0 = -\gamma^0\gamma^i. \quad (119)$$

In the Dirac basis, they have the form:

$$\gamma^0 = \begin{pmatrix} 1 & 0 \\ 0 & -1 \end{pmatrix}, \quad \gamma^a = \begin{pmatrix} 0 & \sigma^a \\ -\sigma^a & 0 \end{pmatrix}, \quad \gamma^5 = \begin{pmatrix} 0 & 1 \\ 1 & 0 \end{pmatrix}. \quad (120)$$

It is often convenient to also define: $\gamma^5 \equiv i\gamma^0\gamma^1\gamma^2\gamma^2$.

Pauli spin matrices:

$$\sigma_x = \begin{pmatrix} 0 & 1 \\ 1 & 0 \end{pmatrix}, \quad \sigma_y = \begin{pmatrix} 0 & -i \\ i & 0 \end{pmatrix}, \quad \sigma_z = \begin{pmatrix} 1 & 0 \\ 0 & -1 \end{pmatrix} \quad (121)$$

$$\sigma_i\sigma_j = i\epsilon_{ijk}\sigma_k + \delta_{ij}, \qquad [\sigma_i, \sigma_j] = 2i\epsilon_{ijk}\sigma_k \quad (122)$$

$$(\boldsymbol{\sigma}\cdot\boldsymbol{a})(\boldsymbol{\sigma}\cdot\boldsymbol{b}) = \boldsymbol{a}\cdot\boldsymbol{b} + i\boldsymbol{\sigma}\cdot(\boldsymbol{a}\times\boldsymbol{b}) \quad (123)$$

Dirac equation (inDirac basis)

Orbitals are written (for spherical potential):

$$\phi_{n\kappa m}(\boldsymbol{r}) = \begin{pmatrix} f_{n\kappa}(r)\,\Omega_{\kappa m}(\boldsymbol{n}) \\ ig_{n\kappa}(r)\,\Omega_{-\kappa,m}(\boldsymbol{n}) \end{pmatrix}, \quad (124)$$

$$\Omega_{\kappa m}(\boldsymbol{n}) = \sum_{\sigma=\pm1/2}\langle l, m-\sigma, 1/2, \sigma|j, m\rangle\, Y_{l,m-\sigma}(\boldsymbol{n})\,\chi_\sigma \quad (125)$$

$$= \begin{pmatrix} (-1)^{j-l-1/2}\sqrt{\frac{\kappa+1/2-m}{2\kappa+1}}Y_{l,m-1/2}(\theta,\phi) \\ \sqrt{\frac{\kappa+1/2+m}{2\kappa+1}}Y_{l,m+1/2}(\theta,\phi) \end{pmatrix} \quad (126)$$

(with $l \equiv |\kappa+1/2| - 1/2$), where

$$\kappa = (l-j)(2j+1), \quad l = |\kappa+1/2| - 1/2, \quad j = |\kappa| - 1/2. \quad (127)$$

The DE can also be written in radial form as

$$\begin{pmatrix} V-\varepsilon & c(-\partial_r + \frac{\kappa}{r}) \\ c(\partial_r + \frac{\kappa}{r}) & V-\varepsilon-2c^2 \end{pmatrix}\begin{pmatrix} f_{n\kappa} \\ g_{n\kappa} \end{pmatrix} = 0. \quad (128)$$

Some useful identities:

$$(\boldsymbol{\sigma}\cdot\boldsymbol{p})y(r)\Omega_{\kappa m} = i\left(y' + \frac{\kappa+1}{r}y\right)\Omega_{-\kappa,m} \quad (129)$$

$$(\boldsymbol{\sigma}\cdot\boldsymbol{n})\Omega_{\kappa m} = -\Omega_{-\kappa,m}, \quad (130)$$

and

$$[\boldsymbol{p}, y]\phi = \phi\,(\boldsymbol{p}y). \quad (131)$$

References

[1] H. A. Bethe and E. E. Salpeter, *Quantum mechanics of one-and two-electron atoms* (Plenum Publishing Corporation, New York, 1977).

[2] I. Lindgren and J. Morrison, *Atomic many-body theory*, 2nd ed. (Springer-Verlag, New York, 1986).

[3] W. R. Johnson, *Atomic Structure Theory* (Springer, New York, 2007).

[4] V. A. Dzuba, O. P. Sushkov, and V. V. Flambaum, Prepr. INP 82-89 **INP 82-89** (1982).

[5] G. B. Arfken, H. J. Weber, and F. E. Harris, *Mathematical Methods for Physicists* (Elsevier, 2013).

[6] A. E. S. Green, D. L. Sellin, and A. S. Zachor, Phys. Rev. **184**, 1 (1969).

[7] V. A. Dzuba, V. V. Flambaum, P. G. Silvestrov, and O. P. Sushkov, Phys. Lett. A **131**, 461 (1988).

[8] V. A. Dzuba, V. V. Flambaum, and O. P. Sushkov, Phys. Lett. A **140**, 493 (1989).

[9] J. C. Slater, Phys. Rev. **81**, 385 (1951).

[10] V. A. Dzuba, V. V. Flambaum, and O. P. Sushkov, J. Phys. B **17**, 1953 (1984).

[11] A. Dalgarno and J. T. Lewis, Proceedings of the Royal Society A **233**, 70 (1955).

[12] V. A. Dzuba, J. C. Berengut, J. S. M. Ginges, and V. V. Flambaum, Phys. Rev. A **98**, 043411 (2018), arXiv:1805.04989 .

[13] N. L. Manakov, V. D. Ovsiannikov, and L. P. Rapoport, Phys. Rep. **141**, 320 (1986).

[14] W. R. Johnson, C. D. Lin, K. T. Cheng, and C. M. Lee, Phys. Scr. **21**, 409 (1980).

[15] W. R. Johnson, Adv. At. Mol. Opt. Phys. **25**, 375 (1989).

[16] W. R. Johnson, S. A. Blundell, and J. Sapirstein, Phys. Rev. A **37**, 307 (1988).

[17] K. Beloy and A. Derevianko, Comput. Phys. Commun. **179**, 310 (2008), arXiv:0710.3142 .

[18] E. V. Kahl and J. C. Berengut, Comput. Phys. Commun. **in press** (2019), 10.1016/j.cpc.2018.12.014, arXiv:1805.11265 .

[19] J. S. M. Ginges and V. V. Flambaum, Phys. Rep. **397**, 63 (2004).

[20] V. V. Flambaum and J. S. M. Ginges, Phys. Rev. A **72**, 052115 (2005).

[21] J. S. M. Ginges and J. C. Berengut, J. Phys. B **49**, 095001 (2016).

[22] J. S. M. Ginges and J. C. Berengut, Phys. Rev. A **93**, 052509 (2016), arXiv:1603.09116 .

[23] L. D. Landau and E. M. Lifshitz, *Quantum Mechanics: Non-relativistic Theory* (Pergamon, Oxford, 1977).

[24] I. I. Sobelman, *Atomic Spectra and Radiative Transitions* (Springer, Berlin, Heidelberg, 1992).

[25] D. A. Varshalovich, A. N. Moskalev, and V. K. Khersonskii, *Quantum Theory of Angular Momentum* (World Scientific, Singapore, 1988).

[26] J. J. Sakurai, *Modern Quantum Mechanics* (2011).